JOM 23418

Versatile ligand behaviour of di-2-pyridylketone 2-aminobenzoylhydrazone (Hdpa) towards $SnPh_2Cl_2$. Crystal structures of $[SnPh_2(Hdpa)Cl_2]$ and $[SnPh(dpa)Cl_2]$ *

Sandra Ianelli, Manuela Orcesi, Corrado Pelizzi, Giancarlo Pelizzi and Giovanni Predieri

Istituto di Chimica Generale e Inorganica, Università di Parma, Centro di Studio per la Strutturistica Diffrattometrica del CNR,
Viale delle Scienze, I-43100 Parma (Italy)

(Received October 6, 1992)

Abstract

From the reaction of di-2-pyridylketone 2-aminobenzoylhydrazone (Hdpa) with $SnPh_2Cl_2$ two complexes, $[SnPh_2(Hdpa)Cl_2]$ (**1**) and $[SnPh(dpa)Cl_2]$ (**2**), were isolated as yellow and red crystalline products, respectively. In compound **1** the Hdpa coordinates very weakly to tin through O (2.434(7) Å), N(1) (2.695(8) Å) and N(3) (2.749(9) Å); on the contrary, in **2** the Hdpa is deprotonated and binds much more strongly to tin through the same atoms (2.200(16), 2.162(19) and 2.140(18) Å, respectively). ^{119}Sn NMR data in dimethyl sulphoxide suggest that the solid state structure of **2** is retained, whereas that of **1** breaks down in solution.

1. Introduction

Our interest in organotin chemistry, aroused by the ability of tin to assume a variety of coordination geometries and to produce cationic, neutral or anionic organotin species [1,2], has been recently focused also on the biological aspects [3].

In connection with previous investigations on the coordinating properties of acylhydrazones [4,5], and in order to isolate new organotin-hydrazone complexes with potential antimicrobial properties, we have synthesized some di-2-pyridylketone acylhydrazones [6].

In this paper we report the synthesis, the IR and ^{119}Sn NMR spectroscopic data and the X-ray crystal structure of two organotin compounds obtained from the reaction of dichlorodiphenyltin with di-2-pyridylketone 2-aminobenzoylhydrazone (Hdpa), namely $[SnPh_2(Hdpa)Cl_2]$ (**1**) and $[SnPh(dpa)Cl_2]$ (**2**).

2. Experimental details

All reactants and solvents were reagent grade. Solvents were dried by standard techniques before use. Dichlorodiphenyltin was purchased from Strem Chemical Co., and di-2-pyridylketone and 2-aminobenzohydrazide from Aldrich.

Microanalyses (C, H and N) were made with Carlo Erba EA 1108 automatic equipment; determination of tin was by atomic absorption spectroscopy using a Perkin Elmer 303-HGA70 instrument. Mass spectra were recorded with a Varian CH-5 spectrometer at 70 eV (*ca.* 1.12×10^{-17} J). FTIR spectra were obtained in the range 4000–400 cm^{-1} using a Nicolet 5PC spectrometer. ^{119}Sn NMR spectra were recorded on a Bruker CXP 200 instrument at 74.5 MHz, using ^2H lock. Chemical shifts are given relative to external $SnMe_4$, negative indicating a shift to high field; $[^2H]$chloroform or $[^2H_6]$dimethyl sulphoxide were used as solvents. The thermogravimetric analysis were made from 30 to 400°C, at a rate of 20° min^{-1} with a Perkin Elmer Delta Series TGA 7 thermobalance. For the calorimetric analysis, a Perkin Elmer DSC 7 instrument was used, from 30 to 300°C at the same heating rate.

Correspondence to: Professor G. Pelizzi.

* Dedicated to Professor Gian Paolo Chiusoli in recognition of his outstanding contributions to organometallic chemistry and homogeneous catalysis and as a mark of friendship.

0022-328X/93/$6.00

2.1. Preparation of the hydrazone, Hdpa

To an absolute ethanol solution of di-2-pyridylketone an equimolar amount of 2-aminobenzohydrazide, dissolved in the same solvent, was added dropwise at room temperature. The resulting solution was then heated under reflux for ca. 4 h with magnetic stirring. Slow evaporation of the solvent at room temperature gave a yellow microcrystalline product identified as Hdpa (yield 85%; m.p. 178°C; m/e 65(22), 78(11), 92(20), 120(21), 169(100), 197(81), 317(7%).

2.2. Preparation of the organotin complexes

An absolute ethanol solution of Hdpa and $SnPh_2Cl_2$ (1 : 1 molar ratio) was heated under reflux for 1 h with magnetic stirring. The reddish orange solution was then cooled and allowed to stand at room temperature. By slow evaporation of the solvent two crystalline products, a yellow (yield 35%) and a red (45%), were isolated, according to the reaction scheme reported below.

$$\mathrm{Hdpa} + \mathrm{SnPh_2Cl_2} \xrightarrow[1:1\ \mathrm{reflux}]{\mathrm{abs.\ EtOH}}$$

$$\times[\mathrm{SnPh_2(Hdpa)Cl_2}] + [\mathrm{SnPh(dpa)Cl_2}]$$

$$(\mathbf{1},\ \mathrm{yellow}) \qquad (\mathbf{2},\ \mathrm{red})$$

Compound **1**, found: C, 53.9; H, 4.0; N, 10.7; Sn, 18.8; calcd. for $C_{30}H_{25}Cl_2N_5OSn$: C, 54.5; H, 3.8; N, 10.6; Sn, 17.9%. Compound **2**, found: C, 48.8; H, 3.5; N, 12.2; Sn, 20.7; calcd. for $C_{24}H_{19}Cl_2N_5OSn$: C, 49.4; H, 3.3; N, 12.0; Sn, 20.4%.

Attempts to prepare the yellow compound separately from the red were unsuccessful. However, for a Sn/Hdpa molar ratio greater than 1, the yield of the red product increases, whereas the contrary occurs when the ratio is less than 1. The excess of the organotin reagent probably favours the deprotonation of the Hdpa.

2.3. X-ray data collection, structure determination and refinement of compounds 1 and 2

All diffraction measurements were carried out at room temperature on a computer-controlled Siemens AED diffractometer employing Ni-filtered Cu Kα radiation. Automatic routines to search for, centre and index reflections, in conjunction with a cell reduction program, led to a primitive orthorhombic cell for **1** and to a primitive monoclinic cell for **2**. The ambiguities in the space groups, *Pnam* or $Pna2_1$ for **1** and $P2/n$ or *Pn* for **2**, were resolved by analysis of intensity statistics. This clearly indicated in both cases the absence of a centre of symmetry and successful models were found with the space groups $Pna2_1$ (**1**) and *Pn* (**2**). The unit-cell dimensions were obtained from the setting angles of 30 (**1**) and 24 (**2**) reflections. They are listed in Table 1, which also contains details of the data collection and structural analysis. No evidence of crystal decomposition or loss of alignment was observed during the course of the experiments. The individual reflection profiles were analysed following a local modification of the Lehmann and Larsen method [7]. The data were corrected for Lorentz, polarization and absorption effects.

TABLE 1. Crystallographic data and data collection and structure analysis summary for compounds **1** and **2**

	1	2
Formula	$C_{30}H_{25}Cl_2N_5OSn$	$C_{24}H_{19}Cl_2N_5OSn$
Molecular weight	661.16	583.04
Crystal system	Orthorhombic	Monoclinic
Space group	$Pna2_1$	*Pn*
a (Å)	8.880(2)	8.762(1)
b (Å)	20.167(7)	9.541(1)
c (Å)	15.888(5)	14.169(2)
α (°)	90	90
β (°)	90	97.91(1)
γ (°)	90	90
V (Å^3)	2845(1)	1173.2(3)
Z	4	2
D_c (g cm^{-1})	1.543	1.650
F(000)	1328	580
μ (cm^{-1})	93.4	112.4
θ range (°)	3–70	3–65
n° of data collected	3089	2227
n° of unique obs. reflections	2130	1716
Max height in final $\Delta\rho$ (e Å^{-3})	0.71	0.84
R	0.0344	0.0795
R_w	0.0432	0.1029

Features common to both determinations include: Cu Kα radiation (λ = 1.54178 Å), θ–2θ scan method and the σ criterion ($I > 2\sigma(I)$).

Both structures were solved by Patterson and Fourier methods and refined by full-matrix least-squares in which all non-hydrogen atoms were treated anisotropically. The quantity minimized was $\Sigma w(|F_o| - |F_c|)^2$ with weighting of the form $w = k/[\sigma^2(F_o) + gF_o^2]$. For the tin atom, the z coordinate in **1** and the x and z coordinates in **2** were fixed to specify the origin in the appropriate space group. For **1**, all the hydrogen atoms, except H(30) which was calculated as riding on its carbon, were found on a difference map and included in the later stages of the refinement with individual isotropic thermal parameters. For **2**, although a difference map revealed electron density at several of the expected hydrogen-atom positions, it was found to be more convenient to include all the hydrogen atoms bonded to the aromatic rings at the calculated riding positions with isotropic group-restrained thermal parameters. The two H's bonded to N(5) were located from a difference map and refined isotropically. In both cases a final difference map showed no anomalous features. Neutral atom scattering factors were employed and the anomalous dispersion terms for the non-hydrogen atoms were included in F_c. Calculations were performed on a Gould Powernode 6040 computer using the SHELX 76 [8], SHELX 86 [9], ABSORB [10], PARST [11] and ORTEP [12] program packages.

Final atomic coordinates are presented in Table 2 for **1** and in Table 3 for **2**. Full lists of atomic coordinates, and thermal parameters have been deposited with the Cambridge Crystallographic Data Centre.

3. Discussion

3.1. X-ray structures

We have previously synthesized some organotin complexes by reaction of organotin chlorides with mono- or bis-(acylhydrazones) and in all cases only one complex species was isolated. However, in the present case we observed the formation of two different organotin acylhydrazone compounds, as well as the influence of the experimental conditions on the reaction yield.

TABLE 2. Atomic coordinates ($\times 10^4$) and equivalent isotropic thermal parameters (Å$^2 \times 10^4$) (one third trace of the diagonalized matrix), with esd's in parentheses for **1**

Atom	x	y	z	U_{eq}
Sn	6367.1(6)	4699.1(2)	2500.0(0)	337(1)
Cl(1)	4952(3)	3718(1)	1936(2)	452(7)
Cl(2)	5401(3)	4423(3)	3921(2)	517(8)
O	7358(9)	5556(4)	3426(4)	417(23)
N(1)	7340(9)	4735(4)	894(5)	379(23)
N(2)	8804(11)	7027(5)	1089(7)	463(33)
N(3)	7882(10)	5771(4)	1847(5)	350(26)
N(4)	7967(10)	6288(4)	2416(7)	390(26)
N(5)	7109(16)	5968(6)	5009(7)	693(44)
C(1)	7534(15)	4165(6)	504(7)	520(38)
C(2)	8295(14)	4084(6)	−228(7)	524(39)
C(3)	8962(13)	4631(6)	−592(7)	542(37)
C(4)	8799(14)	5242(5)	−200(7)	481(34)
C(5)	8002(10)	5278(5)	543(5)	328(25)
C(6)	7977(10)	5886(5)	1056(5)	327(26)
C(7)	8077(13)	6551(5)	645(7)	358(31)
C(8)	7430(14)	6668(5)	−143(7)	455(34)
C(9)	7558(16)	7302(7)	−491(9)	634(45)
C(10)	8331(18)	7784(6)	−48(9)	641(48)
C(11)	8909(16)	7633(6)	723(10)	582(48)
C(12)	7831(11)	6117(5)	3239(6)	334(28)
C(13)	8252(11)	6604(5)	3878(7)	371(30)
C(14)	9072(15)	7190(5)	3650(8)	491(40)
C(15)	9519(17)	7636(7)	4227(9)	578(45)
C(16)	9183(17)	7519(7)	5069(11)	621(52)
C(17)	8407(22)	6989(9)	5301(10)	616(54)
C(18)	7917(15)	6493(7)	4734(7)	464(39)
C(19)	8466(10)	4208(4)	2622(8)	327(27)
C(20)	9829(10)	4540(5)	2497(11)	489(28)
C(21)	11179(12)	4182(5)	2546(16)	590(34)
C(22)	11190(12)	3505(6)	2663(10)	581(46)
C(23)	9841(14)	3188(6)	2760(11)	777(59)
C(24)	8501(12)	3525(5)	2729(10)	627(56)
C(25)	4621(11)	5364(4)	2146(6)	351(27)
C(26)	4055(12)	5355(5)	1341(7)	463(32)
C(27)	2775(14)	5732(6)	1140(8)	551(40)
C(28)	2102(14)	6126(7)	1739(9)	606(45)
C(29)	2688(11)	6141(5)	2524(12)	568(32)
C(30)	3935(11)	5760(5)	2757(7)	474(36)

TABLE 3. Atomic coordinates ($\times 10^4$) and equivalent isotropic thermal parameters (Å$^2 \times 10^4$) (one third trace of the diagonalized matrix), with esd's in parentheses for **2**

Atom	x	y	z	U_{eq}
Sn	2500	1222(1)	2500	454(4)
O	399(17)	144(16)	2797(13)	571(55)
Cl(1)	3862(8)	−143(6)	3846(5)	640(20)
Cl(2)	1080(8)	2181(6)	1033(5)	623(20)
N(1)	4593(20)	1173(17)	1851(13)	471(55)
N(2)	3871(28)	−2047(23)	−277(16)	669(81)
N(3)	2406(20)	−697(19)	1711(14)	451(55)
N(4)	1147(24)	−1531(20)	1740(15)	545(65)
N(5)	−1904(31)	−728(27)	3834(24)	900(106)
C(1)	5672(30)	2145(24)	1979(20)	612(89)
C(2)	7009(31)	2020(26)	1573(19)	596(82)
C(3)	7219(35)	893(31)	981(23)	718(103)
C(4)	6100(36)	−103(33)	895(26)	740(128)
C(5)	4774(27)	43(21)	1292(15)	466(66)
C(6)	3443(24)	−991(21)	1206(18)	503(70)
C(7)	3464(26)	−2252(26)	607(20)	570(81)
C(8)	3135(33)	−3591(20)	924(23)	647(91)
C(9)	3227(34)	−4708(29)	344(27)	823(127)
C(10)	3633(45)	−4541(41)	−551(31)	1040(168)
C(11)	3923(39)	−3193(33)	−818(24)	773(109)
C(12)	185(29)	−1022(22)	2320(18)	528(73)
C(13)	−1161(25)	−1886(24)	2387(19)	513(75)
C(14)	−1599(35)	−2925(42)	1735(27)	762(120)
C(15)	−2690(32)	−3841(34)	1800(25)	780(110)
C(16)	−3674(33)	−3653(25)	2487(24)	684(97)
C(17)	−3387(33)	−2690(28)	3137(21)	566(87)
C(18)	−2111(29)	−1695(23)	3146(19)	545(77)
C(19)	2723(28)	3205(21)	3289(17)	466(69)
C(20)	1802(35)	4393(24)	2920(19)	654(93)
C(21)	2070(36)	5688(29)	3386(22)	704(104)
C(22)	3156(37)	5783(22)	4195(22)	687(103)
C(23)	4064(37)	4701(27)	4522(23)	767(111)
C(24)	3845(38)	3336(25)	4096(19)	645(93)

An ORTEP view of the molecular structures showing the atomic numbering schemes is given in Fig. 1 for **1** and in Fig. 2 for **2**. Bond distances and angles are listed in Tables 4 and 5 for **1** and **2**, respectively. The main structural differences between the two compounds are related to the behaviour of the hydrazone molecule. In **1** it is neutral and coordinates very weakly to tin through O, which is at 2.434(7) Å, and N(1) and N(3), which are more remotely attached at 2.695(8) and 2.749(9) Å from the tin, respectively; in contrast, in **2** the Hdpa is deprotonated and binds strongly to tin through the above three atoms (Sn–O 2.200(16), Sn–N(1) 2.162(19), Sn–N(3) 2.140(18) Å). Moreover, when the hydrazone is neutral as in **1**, the formation of an intramolecular hydrogen bond causes the N(2)–C(11)

TABLE 4. Bond distances (Å) and angles (°) with esd's in parentheses for **1**

Sn–Cl(1)	2.509(3)	C(8)–C(9)	1.397(17)
Sn–Cl(2)	2.479(3)	C(9)–C(10)	1.384(19)
Sn–O	2.434(7)	C(10)–C(11)	1.363(21)
Sn–C(19)	2.120(8)	C(12)–C(13)	1.461(14)
Sn–C(25)	2.126(9)	C(13)–C(14)	1.434(15)
O–C(12)	1.241(12)	C(13)–C(18)	1.410(16)
N(1)–C(1)	1.316(14)	C(14)–C(15)	1.344(19)
N(1)–C(5)	1.363(12)	C(15)–C(16)	1.392(22)
N(2)–C(7)	1.355(15)	C(16)–C(17)	1.325(24)
N(2)–C(11)	1.356(16)	C(17)–C(18)	1.413(22)
N(3)–N(4)	1.381(13)	C(19)–C(20)	1.398(13)
N(3)–C(6)	1.280(12)	C(19)–C(24)	1.387(13)
N(4)–C(12)	1.359(14)	C(20)–C(21)	1.402(14)
N(5)–C(18)	1.352(18)	C(21)–C(22)	1.377(17)
C(1)–C(2)	1.355(17)	C(22)–C(23)	1.366(17)
C(2)–C(3)	1.380(17)	C(23)–C(24)	1.372(16)
C(3)–C(4)	1.389(16)	C(25)–C(26)	1.373(14)
C(4)–C(5)	1.378(14)	C(25)–C(30)	1.397(14)
C(5)–C(6)	1.472(13)	C(26)–C(27)	1.405(16)
C(6)–C(7)	1.495(14)	C(27)–C(28)	1.377(19)
C(7)–C(8)	1.398(16)	C(28)–C(29)	1.351(23)
		C(29)–C(30)	1.398(15)
C(19)–Sn–C(25)	163.8(4)	N(2)–C(11)–C(10)	124.2(12)
O–Sn–C(25)	88.6(3)	O–C(12)–N(4)	119.4(9)
O–Sn–C(19)	87.6(3)	N(4)–C(12)–C(13)	118.4(8)
Cl(2)–Sn–C(25)	97.5(3)	O–C(12)–C(13)	122.2(9)
Cl(2)–Sn–C(19)	96.6(3)	C(12)–C(13)–C(18)	120.6(9)
Cl(2)–Sn–O	74.6(2)	C(12)–C(13)–C(14)	120.6(10)
Cl(1)–Sn–C(25)	92.1(3)	C(14)–C(13)–C(18)	118.7(10)
Cl(1)–Sn–C(19)	96.0(2)	C(13)–C(14)–C(15)	121.9(12)
Cl(1)–Sn–O	163.1(2)	C(14)–C(15)–C(16)	118.6(13)
Cl(1)–Sn–Cl(2)	88.6(1)	C(15)–C(16)–C(17)	121.1(16)
Sn–O–C(12)	128.7(6)	C(16)–C(17)–C(18)	123.6(15)
C(1)–N(1)–C(5)	116.9(9)	C(13)–C(18)–C(17)	116.0(12)
C(7)–N(2)–C(11)	116.5(11)	N(5)–C(18)–C(17)	120.7(12)
N(4)–N(3)–C(6)	120.1(9)	N(5)–C(18)–C(13)	123.2(11)
N(3)–N(4)–C(12)	115.7(8)	Sn–C(19)–C(24)	119.6(7)
N(1)–C(1)–C(2)	125.1(11)	Sn–C(19)–C(20)	121.6(6)
C(1)–C(2)–C(3)	118.5(11)	C(20)–C(19)–C(24)	118.3(8)
C(2)–C(3)–C(4)	118.5(11)	C(19)–C(20)–C(21)	119.0(9)
C(3)–C(4)–C(5)	119.0(10)	C(20)–C(21)–C(22)	121.6(10)
N(1)–C(5)–C(4)	122.0(9)	C(21)–C(22)–C(23)	118.2(11)
C(4)–C(5)–C(6)	121.8(9)	C(22)–C(23)–C(24)	121.7(11)
N(1)–C(5)–C(6)	115.8(8)	C(19)–C(24)–C(23)	121.0(10)
N(3)–C(6)–C(5)	113.2(8)	Sn–C(25)–C(30)	119.6(7)
C(5)–C(6)–C(7)	120.3(8)	Sn–C(25)–C(26)	120.3(7)
N(3)–C(6)–C(7)	126.5(9)	C(26)–C(25)–C(30)	119.7(9)
N(2)–C(7)–C(6)	115.9(9)	C(25)–C(26)–C(27)	120.0(10)
C(6)–C(7)–C(8)	121.2(9)	C(26)–C(27)–C(28)	120.5(11)
N(2)–C(7)–C(8)	122.9(10)	C(27)–C(28)–C(29)	118.8(12)
C(7)–C(8)–C(9)	118.3(11)	C(28)–C(29)–C(30)	122.6(14)
C(8)–C(9)–C(10)	118.9(12)	C(25)–C(30)–C(29)	118.3(11)
C(9)–C(10)–C(11)	119.1(12)		

pyridine ring to assume the orientation assumed in the free state [13], unlike what is observed in **2**.

The different bonding mode of the hydrazone is also reflected in the geometry of the coordination polyhedron. In **1** the tin atom has seven-fold coordination with four close (two phenyl C and two Cl) and three distant (see above) atoms forming a highly irregular environment which cannot be adequately described by any idealized geometry. In **2** the tin coordination sphere is more regular and involves a phenyl C and two Cl atoms which are mutually trans in addition to the three hydrazone atoms leading to a distorted octahedral environment. As a result of the chelating action of dpa, the angle O–Sn–N(1) is 148.5(6)°, the principal deviation from idealized octahedral geometry.

Compared with **1**, the Sn–Cl bond distances in **2** are slightly shorter and are fairly consistent with those observed for other six-coordinated organotin(IV) compounds containing *trans*-chlorines (*e.g.* 2.493(1) and 2.507(1) Å in (2,2′-bipyridyl)dichlorobis(*p*-tolyl)tin [14] and 2.475(2) and 2.509(2) Å in *cis*-dichlorobis(*p*-chlorophenyl)(4,4′-dimethyl-2,2′-bipyridyl-*N*,*N*′)tin toluene clathrate [15]. The Sn–N bond distances in **2** are relatively short compared to those found in the

TABLE 5. Bond distances (Å) and angles (°) with esd's in parentheses for **2**

Sn–Cl(1)	2.476(6)	C(5)–C(6)	1.519(30)
Sn–Cl(2)	2.448(6)	C(6)–C(7)	1.475(34)
Sn–O	2.200(16)	C(7)–C(8)	1.397(33)
Sn–N(1)	2.162(19)	C(8)–C(9)	1.355(41)
Sn–N(3)	2.140(18)	C(9)–C(10)	1.373(60)
Sn–C(19)	2.193(21)	C(10)–C(11)	1.375(51)
O–C(12)	1.301(27)	C(12)–C(13)	1.453(33)
N(1)–C(1)	1.319(30)	C(13)–C(14)	1.373(45)
N(1)–C(5)	1.361(27)	C(13)–C(18)	1.460(38)
N(2)–C(7)	1.363(37)	C(14)–C(15)	1.307(47)
N(2)–C(11)	1.340(39)	C(15)–C(16)	1.398(48)
N(3)–N(4)	1.366(27)	C(16)–C(17)	1.301(40)
N(3)–C(6)	1.263(31)	C(17)–C(18)	1.465(37)
N(4)–C(12)	1.346(34)	C(19)–C(20)	1.447(33)
N(5)–C(18)	1.336(38)	C(19)–C(24)	1.407(36)
C(1)–C(2)	1.380(40)	C(20)–C(21)	1.405(37)
C(2)–C(3)	1.392(41)	C(21)–C(22)	1.389(41)
C(3)–C(4)	1.358(44)	C(22)–C(23)	1.346(38)
C(4)–C(5)	1.366(43)	C(23)–C(24)	1.437(36)
N(3)–Sn–C(19)	176.9(8)	N(3)–C(6)–C(5)	114.5(19)
N(1)–Sn–C(19)	102.4(7)	C(5)–C(6)–C(7)	120.4(19)
N(1)–Sn–N(3)	74.5(7)	N(3)–C(6)–C(7)	125.1(20)
Cl(2)–Sn–C(19)	96.3(6)	N(2)–C(7)–C(6)	115.9(21)
Cl(2)–Sn–N(3)	84.1(5)	C(6)–C(7)–C(8)	122.8(24)
Cl(2)–Sn–N(1)	90.5(5)	N(2)–C(7)–C(8)	121.2(23)
Cl(1)–Sn–C(19)	93.5(6)	C(7)–C(8)–C(9)	119.5(26)
Cl(1)–Sn–N(3)	86.1(5)	C(8)–C(9)–C(10)	120.9(28)
Cl(1)–Sn–N(1)	88.2(5)	C(9)–C(10)–C(11)	116.4(35)
Cl(1)–Sn–Cl(2)	170.2(2)	N(2)–C(11)–C(10)	125.7(32)
O–Sn–C(19)	108.9(8)	O–C(12)–N(4)	124.6(20)
O–Sn–N(3)	74.2(6)	N(4)–C(12)–C(13)	114.6(20)
O–Sn–N(1)	148.5(6)	O–C(12)–C(13)	120.8(20)
O–Sn–Cl(2)	89.8(5)	C(12)–C(13)–C(18)	121.8(21)
O–Sn–Cl(1)	86.2(5)	C(12)–C(13)–C(14)	121.4(24)
Sn–O–Cl(2)	111.4(14)	C(14)–C(13)–C(18)	116.8(23)
Sn–N(1)–C(5)	116.0(14)	C(13)–C(14)–C(15)	125.0(33)
Sn–N(1)–C(1)	124.1(15)	C(14)–C(15)–C(16)	119.4(30)
C(1)–N(1)–C(5)	119.9(20)	C(15)–C(16)–C(17)	120.4(28)
C(7)–N(2)–C(11)	116.3(24)	C(16)–C(17)–C(18)	122.5(27)
Sn–N(3)–C(6)	120.4(15)	C(13)–C(18)–C(17)	115.1(22)
Sn–N(3)–N(4)	117.1(14)	N(5)–C(18)–C(17)	118.8(24)
N(4)–N(3)–C(6)	122.3(19)	N(5)–C(18)–C(13)	126.1(23)
N(3)–N(4)–C(12)	112.6(18)	Sn–C(19)–C(24)	119.6(16)
N(1)–C(1)–C(2)	121.0(22)	Sn–C(19)–C(20)	119.1(17)
C(1)–C(2)–C(3)	120.6(25)	C(20)–C(19)–C(24)	121.1(20)
C(2)–C(3)–C(4)	116.2(28)	C(19)–C(20)–C(21)	118.1(24)
C(3)–C(4)–C(5)	122.4(28)	C(20)–C(21)–C(22)	119.8(25)
N(1)–C(5)–C(4)	119.7(21)	C(21)–C(22)–C(23)	122.6(25)
C(4)–C(5)–C(6)	126.0(22)	C(22)–C(23)–C(24)	120.8(28)
N(1)–C(5)–C(6)	114.3(18)	C(19)–C(24)–C(23)	117.4(24)

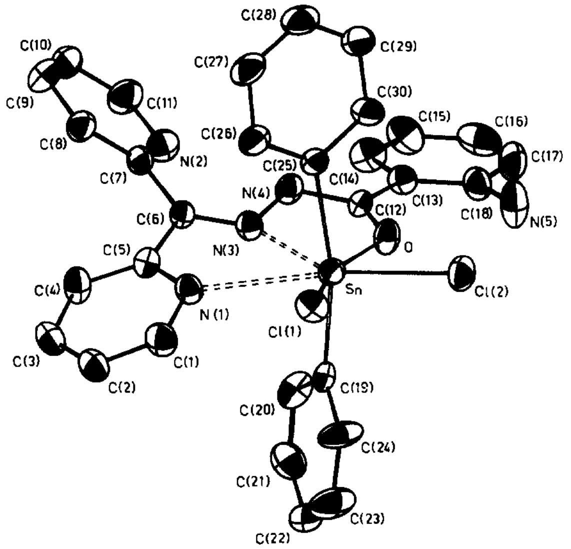

Fig. 1. ORTEP diagram and atom labelling scheme for compound **1**. Thermal ellipsoids are drawn at the 40% probability level.

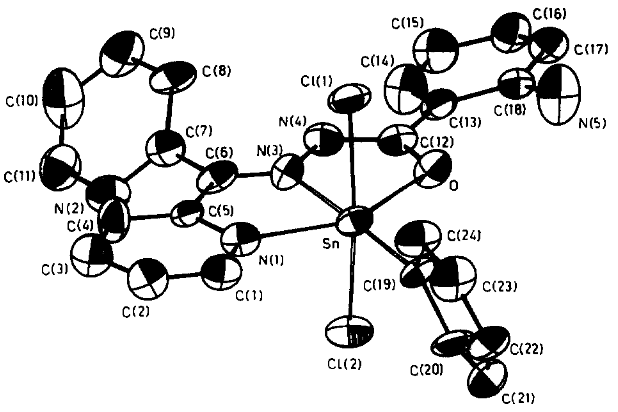

Fig. 2. ORTEP diagram and atom labelling scheme for compound **2**. Thermal ellipsoids are drawn at the 40% probability level.

other structurally characterized tin(IV)-hydrazone derivatives (all of which are seven-coordinate), whereas the Sn–O bond distance lies in the range observed for the above compounds (Sn–N 2.193–2.356 Å; Sn–O 2.096–2.285 Å) [1,16].

By virtue of coordinative interactions, hydrogen bonding and steric hindrance, the configuration the hydrazone assumes in the two compounds is different as indicated by the dihedral angles between the planes defined below.

ring [N(1),C(1)–C(5)] and ring [N(2),C(7)–C(11)]	57.6(3)° in **1**	48.4(9)° in **2**
ring [N(1),C(1)–C(5)] and chain [C(6)N(3)N(4)C(12)O]	26.1(3)	4.0(7)
ring [N(2),C(7)–C(11)] and chain [C(6)N(3)N(4)C(12)O]	31.5(3)	44.8(9)
ring [C(13)–C(18)] and chain [C(6)N(3)N(4)C(12)O]	15.0(5)	14.7(8)

We conclude that the hydrazone moiety can be described in terms of four near-planar parts, the three aromatic rings and the CNNCO chain in **1**, and in terms of three near-planar parts in **2**, as the atoms belonging to the N(1)–C(5) ring and to the chain are nearly coplanar.

Significant differences between the two structures also concern hydrogen bonding and molecular packing. In **1** the hydrogen atoms attached to the two N atoms are all involved in hydrogen bonding to different degrees. There are two strong intramolecular hydrogen bonds and a rather weak intermolecular hydrogen bond: N(4) ··· N(2) 2.69(1) Å, N(4)–H ··· N(2) 132°; N(5) ··· O 2.66(1) Å, N(5)–H ··· O 156°; N(5) ··· Cl(1) $(1-x, 1-y, 1/2+z)$ 3.62(1) Å, N(5)–H ··· Cl(1) 155°. The closest intermolecular contact is 3.38(2) Å, between C(11) and C(28) at $x-1/2, 3/2-y, z$.

In **2**, where only N(5) bears hydrogen, one hydrogen bond appears to be bifurcated [N(5) ··· O 2.78(3) Å, N(5)–H ··· O 111°; N(5) ··· N(2) $(x-1/2, -y, z+1/2)$ 2.97(3) Å, N(5)–H ··· N(2) 107°], while the other points towards Cl(1) at $x-1, y, z$ [N(5) ··· Cl(1) 3.75(3) Å]. None of the intermolecular contacts is less than 3.3 Å; the closest approaches are C(8) ··· C(16) $(1+x, y, z)$ 3.32(4) Å and C(4) ··· C(13) $(1+x, y, z)$ 3.42(4) Å.

3.2. Spectroscopic and thermal measurements

Table 6 gives the main vibrational bands of Hdpa in its free state and in the two tin compounds. The spectroscopic patterns in the three cases are fully comparable, even if more marked similarities exist between the spectrum of the free Hdpa and that of compound **1**, where the hydrazone is neutral and participates in the tin coordination more weakly than in **2**.

^{119}Sn NMR chemical shifts provide an effective diagnostic of different structures of such compounds, as

TABLE 6. Main vibrational bands (cm^{-1}) of Hdpa, [SnPh$_2$(Hdpa)Cl$_2$] (**1**) and [SnPh(dpa)Cl$_2$] (**2**)

	ν(NH)	ν(CH)$_{\text{ring}}$	Amide I	ν(CN)	Amide II
Hdpa	3460m br 3370s	3068m	1664vs	1615s 1590sh 1580s	1544m
1	3458m br 3344m	3055m	1625m	1610m 1584s	1545m
2	3480m br 3380s	3085m	1617s	1606m 1585ms	1565m

tin shielding is strongly dependent on the bonding environment. The most important feature of $\delta(^{119}Sn)$ is that an increase in coordination number of the tin atom from four to five or six or seven usually produces an increase in shielding and hence a large upfield shift. Consequently, the different coordination numbers give rise to different ranges of δ [1,17]. The ^{119}Sn NMR chemical shifts (δ, -449 in dmso and -445 ppm in $CHCl_3$) of the six-coordinate tin complex **2** containing dpa, are in the range typical of six-coordination normally observed for phenyltin compounds. Furthermore, the coincidence of the values in a non-coordinating solvent (chloroform) and in a coordinating solvent (dimethyl sulphoxide) strongly suggests that the solid-state structure is also retained in solution. In contrast it appears that the solid-state structure of **1** breaks down in solution as the tin chemical shift value in dimethyl sulphoxide (-405 ppm) is practically the same as that of $SnPh_2Cl_2$ alone (-402 ppm) in the same solvent.

A thermogravimetric analysis (TGA) in the range 30–400°C on compound **1** revealed the loss of a benzene molecule at about 235°C and the occurrence of a gradual decomposition of the sample at *ca.* 250°C. In the differential scanning calorimetric (DSC) experiment a heat loss occurred at 236°C. The product obtained after thermal treatment at this temperature was recognized as compound **2** by elemental analysis and IR spectroscopy.

Acknowledgments

This work was supported by Ministero dell'Università e della Ricerca Scientifica e Tecnologica (40%). The facilities of Centro Interfacoltà di Misure of the University of Parma were used for recording NMR and mass spectra.

References

1 C. Carini, G. Pelizzi, P. Tarasconi, C. Pelizzi, K. C. Molloy and P. C. Waterfield, *J. Chem. Soc., Dalton Trans.*, (1989) 289.

2 M. Carcelli, C. Ferrari, C. Pelizzi, G. Pelizzi, G. Predieri and C. Solinas, *J. Chem. Soc., Dalton Trans.*, (1992) 2127.

3 P. Mazza, M. Orcesi, C. Pelizzi, G. Pelizzi, G. Predieri and F. Zani, *J. Inorg. Biochem.*, *48* (1992) 255.

4 A. Bonardi, C. Merlo, C. Pelizzi, G. Pelizzi, P. Tarasconi and F. Cavatorta, *J. Chem. Soc., Dalton Trans.*, (1991) 1063.

5 S. Ianelli, G. Minardi, C. Pelizzi, G. Pelizzi, L. Reverberi, C. Solinas and P. Tarasconi, *J. Chem. Soc., Dalton Trans.*, (1991) 2113.

6 A. Bacchi, L. P. Battaglia, M. Carcelli, C. Pelizzi, G. Pelizzi, C. Solinas and M. A. Zoroddu, *J. Chem. Soc., Dalton Trans.*, in press.

7 M. S. Lehmann and F. K. Larsen, *Acta Crystallogr., Sect. A, 30* (1974) 580.

8 G. M. Sheldrick, *Program for Crystal Structure Determination*, University of Cambridge, 1976.

9 G. M. Sheldrick, *Program for Structure Solution*, University of Göttingen, 1986.

10 F. Ugozzoli, *Comput. Chem.*, *11* (1987) 109.

11 M. Nardelli, *Comput. Chem.*, *7* (1983) 95.

12 C. K. Johnson, Rep. ORNL-5138, Oak Ridge National Laboratory, Oak Ridge, TN, 1976.

13 G. Pelizzi, unpublished results.

14 V. G. Kumar Das, Wei Chen, C. K. Yap and T. C. W. Mark, *J. Organomet. Chem.*, *299* (1986) 41.

15 V. G. Kumar Das, C. K. Yap, Wei Chen, P. J. Smith and T. C. W. Mark, *J. Chem. Soc., Dalton Trans.*, (1987) 129.

16 D. Delledonne, G. Pelizzi and C. Pelizzi, *Acta Crystallogr., Sect. C, 43* (1987) 1502.

17 B. Wrackmayer, *Annu. Rep. NMR Spectrosc.*, *16* (1985) 73.